Development of a 3D Printed Loop Heat Pipe

Bradley Richard, William G. Anderson, Joel Crawmer
Advanced Cooling Technologies, Inc.
1046 New Holland Ave.
Lancaster, PA USA
bradley.richard@1-act.com

Abstract

CubeSats and Smallsats have increased in popularity and capability, but advanced thermal solutions are required to keep up with the increasing heat loads. Loop heat pipes (LHPs) are a passive solution capable of transporting heat from electronics to deployable radiator panels, but are currently cost prohibitive for most small satellite applications. A 3D printed LHP has been developed using a direct metal laser sintering (DMLS) process. The additive manufacturing process significantly reduces fabrication costs by eliminating labor intensive steps while also eliminating the knife-edge seal to offer improved reliability. The 3D printed wick for the LHP evaporator was developed through an experimental optimization study. A proof of concept LHP was built and tested using a 3D printed primary wick. A maximum power of 125W was achieved during steady state testing. Additional tests were completed including power cycles, adverse elevation, and low power startup. Based on the successful prototype testing additional work is underway for further optimization of the 3D printed wick design and development of DMLS parameters for secondary wick fabrication.

Keywords

Loop Heat Pipe, Additive Manufacturing, Wick, CubeSats, Thermal Management

Nomenclature

P_b : Bubble point pressure (Pa)
R_p : Pore radius (m)
σ : Surface tension (N/m)

1. Introduction

CubeSats and SmallSats have become widely used due to their low costs, fast development times, and increases in capabilities with advanced electronics and deployable mechanisms. The increase in capabilities for compact satellites, however, also results in higher heat loads which require an advanced thermal management solution beyond the use of high thermal conductivity materials for heat spreading. Loop heat pipes (LHPs) are a passive solution which are capable of transporting heat from electronics to deployable radiators, but they are currently cost prohibitive for most CubeSat and SmallSat applications. The use of a 3D printed wick has the potential to significantly reduce LHP fabrication costs while also improving long term reliability. The use of a DMLS fabrication process can eliminate multiple labor-intensive fabrication steps including machining vapor grooves in the primary wick and wick insertion into an aluminum saddle. The ability to print solid and porous wick material together in a single part eliminates the need for the conventional knife-edge seal which improves reliability.

LHPs are passive devices capable of high thermal conductances across long distances. A schematic of an LHP is provided in Figure 1. Heat enters the evaporator and vaporizes the working fluid. The vapor passes through grooves in the primary wick and through the vapor line to the condenser. Here the vapor is condensed and subcooled. The subcooled liquid passes through the bayonet tube into the center of the primary wick. A secondary wick allows for communication between the compensation chamber and center of the primary wick. The compensation chamber contains saturated fluid at a lower pressure than the evaporator which provides the driving force for fluid flow. The capillary pressure of the primary wick must be greater than the total pressure drop of the system to pump liquid from the liquid line return to the evaporation site at the vapor grooves. [1]

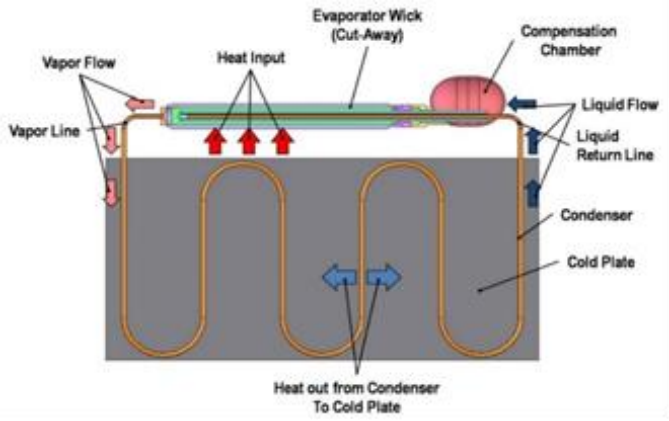

Figure 1: Loop heat pipe schematic (not to scale).

The performance of an LHP primary wick depends largely on pore size. The capillary pressure of a wick is inversely proportional to pore radius. For successful LHP operation the capillary pressure must be greater than the total system pressure drop. Therefore, by reducing the pore size of the primary wick the maximum power can be increased. Traditionally sintered primary wicks have a pore radius of approximately 1µm. DMLS has been demonstrated to be able of printing porous lattice structures, but the smallest pore size to date has been about 50µm. This is due to the accuracy and precision of the laser as well as thermal stresses and heat spreading.

In this work a different approach was taken towards 3D printed wick structures. Instead of building a defined lattice structure, the laser power, speed, and spacing was varied to partially sinter the metal powder together instead of fully

melting the particles. This results in a wick structure very similar to that of traditionally sintered wicks.

2. Experimental Methods

An experimental optimization study was completed by printing a total of 15 samples using a range of DMLS parameters. The goal was to achieve the smallest possible pore size to maximize capillary pumping power. For an LHP the capillary pressure in the primary wick must overcome the total pressure drop of the loop. Each sample was 2.54cm in length and 1.27cm in diameter. Each sample was printed using 316LSS on an EOSINT M280 machine. The parameters which were varied between samples includes laser power, speed, and spacing. By varying these parameters, the metal powder can be sintered together without forming a fully dense part leaving pores for fluid flow.

The pore size of each sample was measured using a bubble test. In the bubble test one side of the wick sample was submerged in methanol while the other side was attached to a pressurized nitrogen line. Methanol is used because it is compatible with stainless steel, and is safer to use for testing than ammonia. The pressure of the nitrogen was slowly increased until nitrogen began to bubble through the wick into the methanol. The pressure where bubbles began to form was recorded and the pore radius was calculated using Eq. 1.

$$r = \frac{2\sigma}{P} \quad (1)$$

where r is the pore radius, σ is the surface tension of the fluid used, and P is the bubble point pressure.

A proof of concept LHP prototype was built as pictured in Figure 2 using a 3D printed primary wick. All wetted parts were 316LSS. The working fluid used was ammonia. The primary wick was 2.54cm in diameter and 10.2cm in length. The primary wick as printed had a porous interior with a fully dense envelope which was welded directly to the compensation chamber and vapor line. The tubing was 0.318cm in diameter and the condenser was 99cm in length. The sink temperature for testing was set to 0°C.

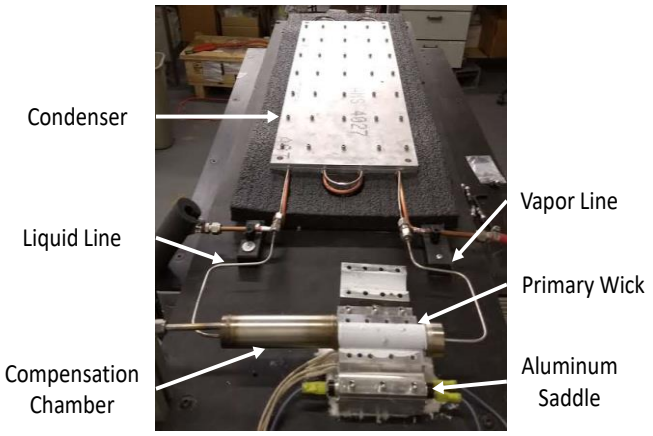

Figure 2: Completed LHP prototype with 3D printed primary wick.

3. Results

The results of the DMLS parameter optimization study are presented in Table 1. The smallest pore size achieved was 5.6μm from sample 2 which is capable of providing enough capillary pressure for an LHP in the 100-300W range. The DMLS parameters for sample 2 were used for fabrication of the LHP prototype. Achieving smaller pore sizes in likely only possible by using smaller diameter metal powder as the base material, but there are no current commercially available solutions.

Sample	Pore Radius (μm)
1	6.2
2	5.6
3	11.6
4	10.3
5	Hollow
6	Solid
7	Solid
8	Solid
9	6.0
10	8.8
11	Hollow
12	31.4
13	20.0
14	13.7
15	29.9

Table 1: Optimization study on DMLS parameters for creating primary wick

The steady state testing results from the LHP prototype are provided in Figure 3. Startup occurred almost instantly at a power of 110W which can be seen by a rapid decrease in the temperature of the liquid line. The power was increased in 5W increments, and steady state was achieved at a maximum power of 125W. At 130W the temperatures of the LHP began to increase linearly which is an indication of dry-out in the primary wick.

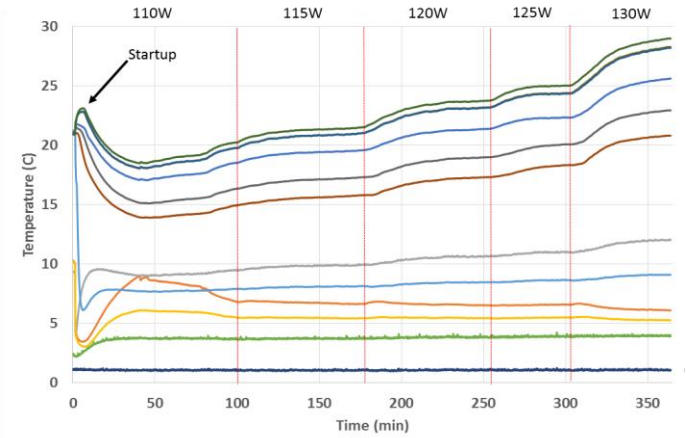

Figure 3: Steady state testing of LHP prototype

A temperature plot of the low power startup test is shown in Figure 4. A power of 5W was applied to the evaporator. The primary wick slowly heated up until there was sufficient superheating of the liquid ammonia in the vapor grooves to

promote boiling. The ability to start the LHP at a power of only 5W indicates that the amount of heat leak is small, because significant heat leak would cause the primary wick and compensation chamber temperatures to increase together preventing LHP operation.

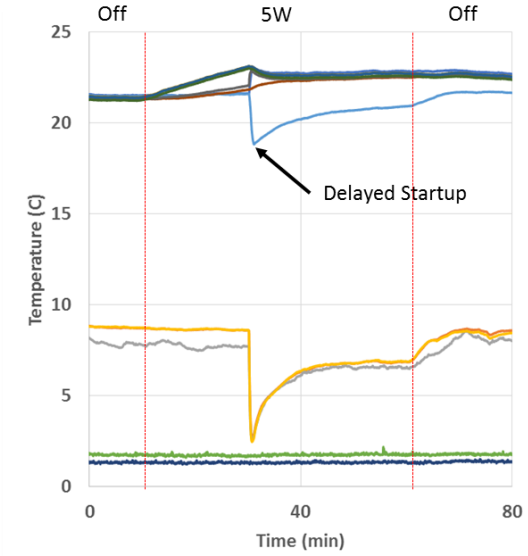

Figure 4: Successful startup of LHP prototype at a heat input of 5W as indicated by the rapid decrease in liquid line temperature.

Testing was completed with the evaporator raised 6in. above the condenser to verify the ability of the LHP to operate against gravity. A temperature plot of the results is presented in Figure 5. Startup and steady state operation were successful at powers of 50W and 70W.

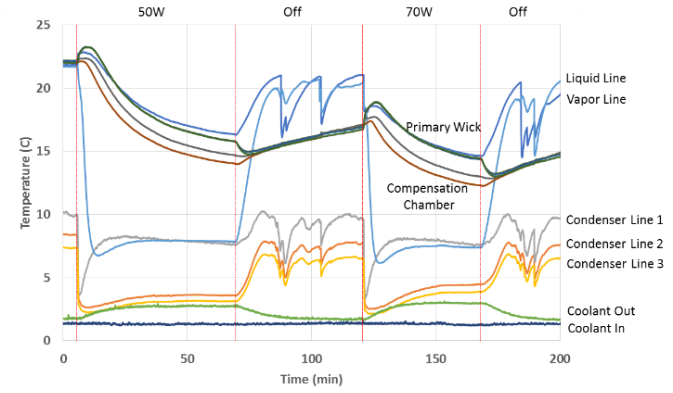

Figure 5: Test results with 6in. of adverse elevation between the evaporator and condenser. Steady state operation was reached at powers of 50W and 70W.

Power cycle testing was completed to verify the ability of the LHP prototype to handle transients. The power was rapidly changed between 70W and 20W. A temperature plot of the results is shown in Figure 6. Dry-out did not occur with rapid increases or decreases in power. This indicates that the secondary wick was able to maintain the supply of liquid to the primary wick during transient operation.

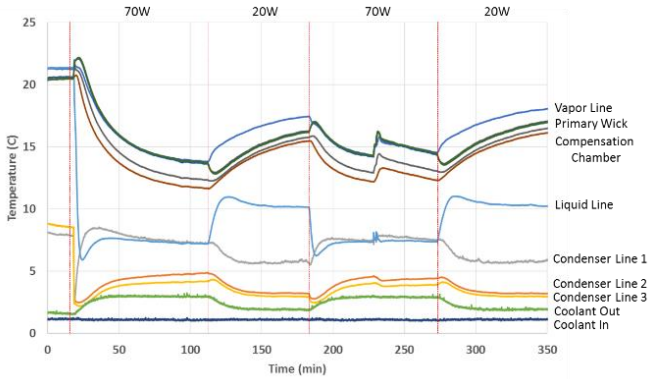

Figure 6: Rapid power cycling between 70W and 20W test results demonstrating the ability of the secondary wick to prevent primary wick dry-out during transients.

4. Conclusions

Significant progress has been made with the development of DMLS parameters for fabricating porous wick materials using 316LSS. An LHP prototype demonstrated the ability of a 3D printed wick to perform as an LHP primary wick. A maximum power of 125W was achieved which is in the power range of current CubeSat technologies. LHP performance was also verified for operation against gravity and during rapid changes in heat input power. Additional work is ongoing to optimize the 3D printed wick design as well as develop DMLS parameters for the secondary wick which has a larger pore size. This will eventually allow for the entire LHP evaporator to be 3D printed which will further reduce cost by eliminating more labor-intensive fabrication steps.

Acknowledgments

This work was funded by NASA through the Small Business Innovation Research (SBIR) program under contract NNX17CM09C. The technical monitor is Dr. Jeff Farmer.

References

1. Ku, Jentung. Operating characteristics of loop heat pipes. No. 1999-01-2007. SAE Technical Paper, 1999.